ChemPubSoc Europe

DOI: 10.1002/ejic.201700935

EurJIC European Journal of Inorganic Chemistry

Full Paper

CLUSTER ISSUE

Magnetic Properties*

Antiferromagnetic Interactions in Copper(II) μ-Oxalato Dinuclear Complexes: The Role of the Counterion

Miguel Julve,*[a] Alain Gleizes,*[b] Lise Marie Chamoreau,[c] Eliseo Ruiz,[d] and Michel Verdaguer*[c]

Dedicated to the memory of the late Professor Olivier Kahn, for his invaluable contributions to the field of molecular magnetism

Abstract: We report the preparation, crystal structure determination, magnetic properties and DFT calculations of five oxalato-bridged dicopper(II) complexes of formula $[Cu_2(bpy)_2(H_2O)_2(C_2O_4)](CF_3SO_3)_2$ (**1**), $[Cu_2(bpy)_2(C_2O_4)](PF_6)_2$ (**2**), $[Cu_2(bpy)_2(C_2O_4)](ClO_4)_2$ (**3**), $[Cu_2(bpy)_2Cl_2(C_2O_4)]\cdot H_2O$ (**4**) and $[Cu_2(bpy)_2(NO_2)_2(C_2O_4)]$ (**5**) (bpy = 2,2′-bipyridine and $C_2O_4^{2-}$ = oxalate). Compounds **1**, **2**, **4** and **5** crystallize in the monoclinic system and **3** crystallizes in the triclinic system. The oxalate ligands in **1**–**5** adopt the bis-bidentate coordination mode and the two bpy molecules act as terminal ligands. The coordination of the counterions and the surroundings of the copper(II) ions differentiate the five compounds. The four nearest neighbours of copper(II) in **1**–**4** are roughly in the plane of the CuC_2O_4Cu framework, whereas they are in an almost perpendicular plane in **5**. Using the isotropic Hamiltonian $\mathbf{H} = -J\,\mathbf{S_1}\cdot\mathbf{S_2}$, where $\mathbf{S_1}$ and $\mathbf{S_2}$ are the spin quantum operators for Cu_1 and Cu_2; J is –384 cm^{-1} for **1**, –392 cm^{-1} for **2** and –387 cm^{-1} for **3**, slightly decreasing to –328 cm^{-1} for **4** and falling to –14 cm^{-1} for **5**. The influence of the anions on the magnetic properties of this family of compounds is explained by the changes in the overlap of the magnetic orbitals through the oxalate bridge. DFT calculations reproduce well the experimental values of J and provide an illustration of the magnetic orbitals.

Introduction

The understanding of the exchange interaction between two spin bearers through multiatomic bridges has made substantial progress in the last few decades.[1–4] Our groups have contributed to these endeavours with the synthesis and the theoretical study of simple dinuclear complexes with bis-bidentate $[XYC_2ZW]^{2-}$ ligands (Scheme 1), such as oxalato (X = Y = Z = W = O),[5–7] oxamato (X = Y = Z = O; W = NH),[8] oxamido (X = Z = O; Y = W = NH),[9,10] dithiooxalato (X = Y = O; Z = W = S),[11] dithiooxamido (X = Z = S; Y = W = NH)[12,13] and tetrathiooxalato (X = Y = Z = W = S).[14]

Mechanisms and exchange pathways have been proposed to explain the large interactions observed in planar TCu^{II}–XYC_2ZW–$Cu^{II}T$ complexes (T, terminal ligand) at various levels of sophistication: semi-empirical;[6] DFT;[15,16] and ab initio.[17] In the simplest two-active-electron model (Scheme 2), the σ-type overlap integral between the localized nonorthogonal magnetic orbitals, a and b, centred on Cu_1 and Cu_2, explains qualitatively the antiferromagnetic coupling through the bridge. The larger the overlap, the wider the energy gap between the two SOMOs, Ψ_1 (u symmetry) and Ψ_2 (g symmetry), built from the ± combination of the a and b magnetic orbitals (Scheme 2b), and the larger the AF coupling. The spin scheme represents the (excited) triplet state.

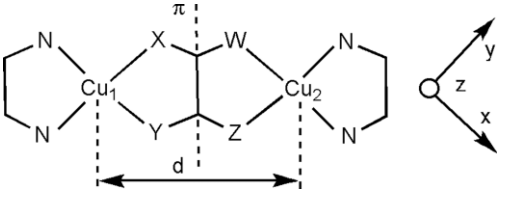

Scheme 1. Dicopper(II) complexes with bis-bidentate oxalate-type ligands and *x,y,z* axes.

When the magnetic orbitals are in the plane of the bridge, they overlap significantly and the interaction is large, even for two copper(II) ions more than 5 Å apart (Scheme 2). When they are in a plane perpendicular to the bridge in complexes with an inversion centre, the overlap is weak (Scheme 3) and the interaction is small (this was called orbital reversal or switching effect by O. Kahn).[18,19]

[a] *Instituto de Ciencia Molecular (ICMol), Universitat de València, 46980 Paterna, Valencia, Spain*
E-mail: miguel.julve@uv.es
https://www.uv.es/qcacoor/
[b] *CIRIMAT, Université de Toulouse, CNRS, INPT, 31030 Toulouse, France*
E-mail: Alain.Gleizes@ensiacet.fr
[c] *Institut Parisien de Chimie Moléculaire, Sorbonne Universités, UPMC Univ Paris 06, Pierre et Marie Curie, 75252 Paris, France*
E-mail: michel.verdaguer@upmc.fr
[d] *Departament de Química Inorgànica i Orgànica and Institut de, Recerca de Química Teòrica i Computacional, Universitat de Barcelona, Diagonal 645, 08028 Barcelona, Spain*

Supporting information and ORCID(s) from the author(s) for this article are available on the WWW under https://doi.org/10.1002/ejic.201700935.

© 2018 Wiley-VCH Verlag GmbH & Co. KGaA, Weinheim

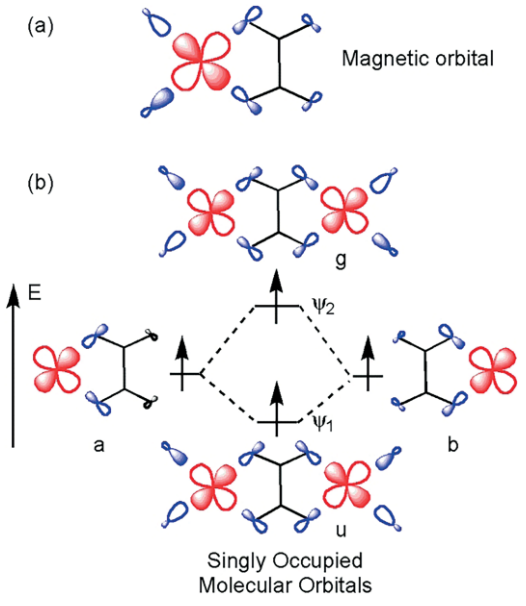

Scheme 2. Schematic representation of: (a) the magnetic orbital of the mononuclear copper(II) complex; and (b) the singly occupied molecular orbitals (SOMOs) in the oxalate-bridged dicopper(II) complex through the σ in-plane exchange pathway.

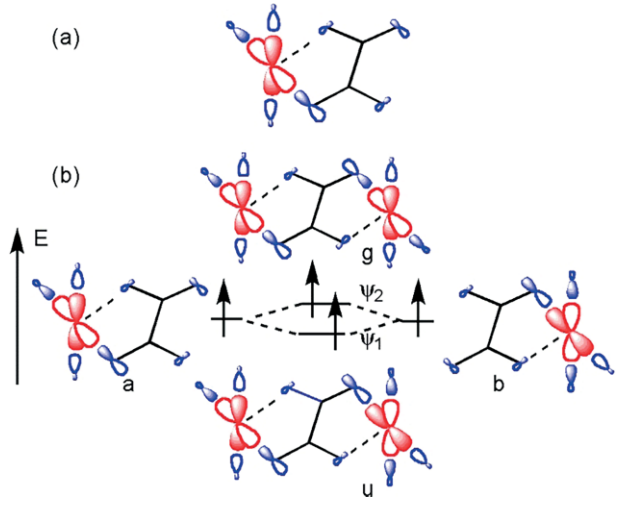

Scheme 3. Schematic representation of: (a) the magnetic orbital perpendicular to the plane of the oxalate ligand; and (b) the SOMOs resulting from the orbital reversal in an oxalate-bridged dicopper(II) complex.

The influence of the nature of the bridging X, Y, Z and W atoms[8,14] and of the terminal ligand T[20] on the exchange interaction has been studied, as well as the exchange pathways in heterobimetallic μ-oxalato complexes, dinuclear species,[21,22] oligonuclear entities,[23] and 1D,[24] 2D or 3D systems.[25–34] Most often, the magnetic properties are in line with simple orbital models.[35–38] The intramolecular ferromagnetism arising from the strict orthogonality of the magnetic orbitals in $[Cu^{II}–V^{IV}O]$,[39] $[Cu^{II}–Cr^{III}]$,[22] $[Ni^{II}–Cr^{III}]$[23] and even $[Cu^{II}–Cu^{II}]$[40] is particularly striking.

We tackle here the unexplored role of the counterion. In most cases, the anion is not (or is very weakly) bound to the metal. It isolates the paramagnetic molecular species from each other and allows the electroneutrality of the framework. It also ensures the stability of the crystal when two complexes of different stoichiometry coexist, as in the case of the compounds of formula $[Cu_2(bpy)_2(H_2O)(C_2O_4)][Cu(bpy)C_2O_4](X)_2$ {X = NO_3^- (**6**), BF_4^- (**7**) and ClO_4^- (**8**)},[41–43] a series of double complexes named after Janus.

On the contrary, in the series of five oxalato-bridged dicopper(II) complexes with 2,2′-bipyridine as the terminal ligand presented here, we show that when the counterion enters the coordination sphere of the copper(II) ion, it strongly modifies the antiferromagnetic coupling from a very strong to a very small value. The ligands and counterions used for the syntheses of complexes **1**–**5** are presented in Scheme 4.

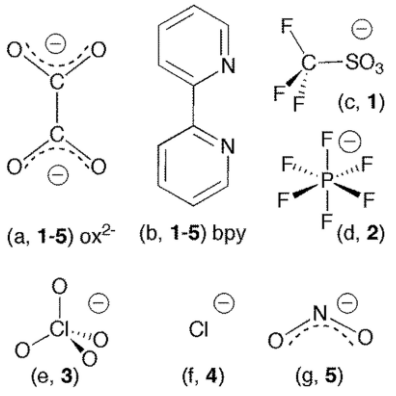

Scheme 4. Ligands and counterions in **1**–**5**.

The magneto-structural results concerning the compounds of formula $[Cu_2(bpy)_2(H_2O)_2(C_2O_4)](CF_3SO_3)_2$ (**1**), $[Cu_2(bpy)_2(C_2O_4)](PF_6)_2$ (**2**), $[Cu_2(bpy)_2(C_2O_4)](ClO_4)_2$ (**3**), $[Cu_2(bpy)_2Cl_2(C_2O_4)]·H_2O$ (**4**) and $[Cu_2(bpy)_2(NO_2)_2(C_2O_4)]$ (**5**) are compared with compounds **6**–**8**[42,43] and also with the previously prepared dinuclear complex $[Cu_2(tmen)_2(H_2O)_2(C_2O_4)](ClO_4)_2·1.25H_2O$ (**9**), which has bidentate *N*,*N*′,*N*″,*N*‴-tetramethylethanediamine (tmen) as the terminal ligand.[5,6]

Results and Discussion

Description of the Structures of 1–5

The structures of compounds **1**–**5** consist of dinuclear (bpy)(L)Cu(μ-C_2O_4)Cu(L)(bpy) entities in which the oxalate groups adopt the bis-bidentate coordination mode, the bpy molecules act as terminal bidentate ligands and L is an additional anionic ligand, L = $CF_3SO_3^-$ (**1**), PF_6^- (**2**), ClO_4^- (**3**), Cl^- (**4**) and NO_2^- (**5**). Selected data for weak bonds, mean planes and the copper surrounding, bond lengths, bond angles and atom–plane distances for **1**–**5** are synoptically displayed in Tables S1–S3. The atom numbering scheme is shown in Figure S1. The plane perpendicular to the oxalate mean plane and comprising the two copper(II) ions is a true mirror plane in **2** and a pseudo one in **1** and **3**–**5**. Each copper(II) in **1** has an axially coordinated water molecule and the two water molecules are *trans* to each other. This water coordination scheme is also observed in complexes **6**–**8**,[41–43] in which the dinuclear [(bpy)(H_2O)Cu(μ-C_2O_4)-

© 2018 Wiley-VCH Verlag GmbH & Co. KGaA, Weinheim

$Cu(H_2O)(bpy)]$ units are cationic with no covalent bonding to the counterions.

The remarkable feature is the variety of geometries triggered by the L ligand, outlined in Figure 1. The dinuclear units have no crystallographically imposed symmetry in the perchlorato derivative **3**, while they have at least one element of symmetry in the other compounds: (i) a twofold axis perpendicular to both the oxalate C–C bond and the Cu–Cu segment in the chloro derivative **4**; (ii) an inversion centre at mid-oxalate C–C bond in the other ones (**1**, **2** and **5**), as in the complexes **6**–**8**,[41–43] and (iii) an inversion centre as the intersection of the true mirror plane with the twofold axis along the oxalate C–C bond in the hexafluorophosphate derivative **2**.

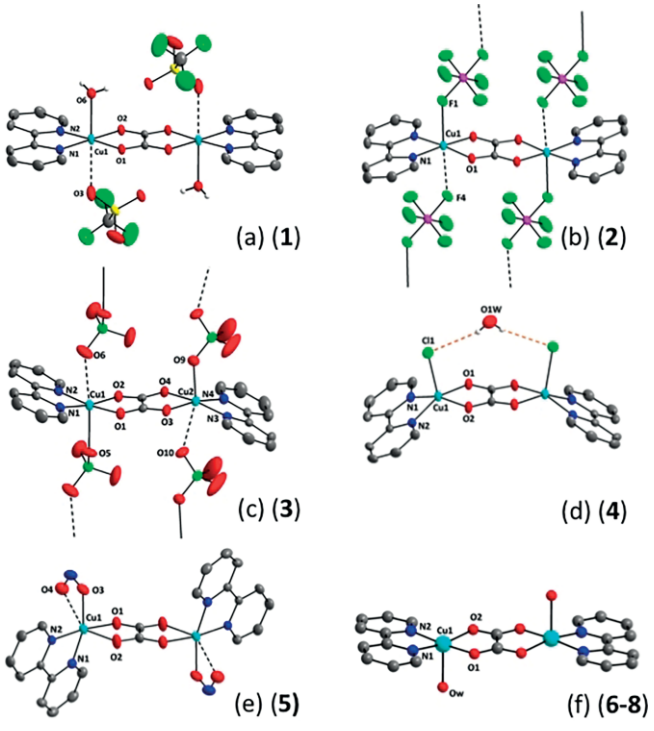

Figure 1. Perspective view of the dinuclear units in compounds **1**–**8**. Colour code: grey (carbon), dark blue (nitrogen), red (oxygen), green (halogen, F or Cl) and pale blue (copper).

The dinuclear (bipy)(L)Cu(μ-C_2O_4)Cu(L)(bipy) entities in compounds **1**–**8** may be divided into three classes, according to the behaviour of the L ligand:

(i) In compounds **4** and **5**, the L ligands are the counterions Cl^- and NO_2^-, respectively; they are bound to the copper(II) ions [Cu–Cl = 2.4468(4) Å (**4**) and Cu–O3 = 2.0055(10) Å (**5**)]. The chlorine atoms in **4** are on the same side of the oxalato bridge and are linked by a doubly H-bonded water molecule (Figure 1d). The nitrito groups in **5** chelate the copper(II) ions in an asymmetric way [Cu–O4 = 2.5402(11) Å]. They are on opposite sides of the oxalato plane (Figure 1e). The copper(II) surrounding in **4** is square pyramidal, whereas it is distorted octahedral in **5**.

(ii) In compounds **1**–**3**, the ligands L are also the counterions, that is, $SO_3CF_3^-$, PF_6^- and ClO_4^-, respectively, but they weakly bind to the copper(II) ions [Cu–O = 2.6813(16) Å (**1**), Cu–F = 2.4347(10) Å (**2**) and Cu–O is from 2.332(13) to 2.380(7) Å (**3**)]. In **1**, a water molecule at 2.3561(11) Å occupies the axial position opposite to the triflate, thus giving a 4 + 1 + 1 octahedral geometry about the copper(II) ions. The triflate ions are *trans* to each other and so are the water molecules. The same 4 + 1 + 1 octahedral geometry arises in **2** and **3** from a very weak interaction between each copper(II) ion and a neighbouring counterion [Cu–F = 2.7351(13) Å (**2**) and Cu–O = 2.7101(24) Å and 2.6589(22) Å (**3**)]. The dinuclear units in **1** are well isolated from each other. However, they build ladders in **2** and **3**, where the (bpy)Cu($O_2C_2O_2$)Cu(bpy) entities are the rods and the PF_6^- or ClO_4^- anions are the rungs (Figures 1b,c).

(iii) The L ligands in the dinuclear entities of the nitrate (**6**), tetrafluoroborate (**7**) and perchlorate (**8**) derivatives are not the counterions. Instead, one water molecule is bound to each of them: Cu–O_w = 2.246(2), 2.279(2) and 2.285(2) Å, respectively. The coordinated water molecules of the dinuclear entity are *trans* to each other, according to the centrosymmetry (Figure 1f). Each copper(II) ion interacts very weakly with a counterion peripheral atom more than 2.7 Å apart, thus achieving a 5 + 1 coordination. The counterion and the water molecule located on the same side of the oxalate plane are hydrogen bonded to each other.

The structures of **6**–**8** are also distinct from **1**–**5** in that they contain both dinuclear and mononuclear entities. In spite of the different counterions, compounds **6**–**8** are isostructural, a feature that has been commented on elsewhere.[42,43]

The shortest Cu–O(oxalate) distances are observed in **1** and **2**. They are strictly equal in **2**, according to the C_{2h} symmetry [Cu–O = 1.9649(8) Å] and they do not differ significantly in **1** [1.9699(8) and 1.9662(8) Å for Cu–O1 and Cu–O2, respectively]. Due to the C_{2h} symmetry, the four basal atoms in **2** are strictly coplanar and the chemically equivalent bonds are equal. The four basal atoms are nearly coplanar (atom–plane distances less than 0.01 Å) in **1**, despite the absence of crystallographically imposed symmetry. These two compounds show the shortest shift of the copper atom from the basal plane [*h* = 0.041(1) (**1**) and 0.079(1) Å (**2**)] and the shortest intramolecular Cu···Cu separation [5.1268(4) (**1**) and 5.1312(5) Å (**2**)].

The two Cu–O(oxalate) distances in **3** and **6**–**8**, although not strictly equal, are similar [1.971(3) ≤ Cu–O1, Cu–O2 ≤ 1.983(2) Å]. The values of the copper–copper separation vary from 5.1521(5) Å in **3** to 5.154(1) Å in **6** and to 5.1846(5) Å in **4**, the largest values being for **1**–**4**. The elevations of the copper(II) ion from the mean basal plane are similar, in the range 0.16–0.18 Å, about twice the value observed in **2**. This parameter jumps to 0.3666(2) Å in **4**, due to the coordinated chloride. Compound **4** has the most wrinkled oxalate group [dihedral angles are 6.0° between the two OOC carboxylate moieties and 5.5° between the O1C1C2 and the C1C2O2′ planes (see Figure S1)], while they are null or less than 1.0° in the other compounds. It also has the largest values of the dihedral angles with the basal plane of the square pyramid (dihedral angles 1 and 2 in Table S2).

The bipyridyl, oxalate and nitrite ligands in **5** are all chelating, a feature that prevents the square-pyramidal coordination of the copper(II) ion. The three chelates coordinate to the metal centre in asymmetrical modes. In particular, the copper–oxalate

© 2018 Wiley-VCH Verlag GmbH & Co. KGaA, Weinheim

bond lengths are quite different [Cu–O1 = 1.9656(8) Å (one of the shortest observed values) and Cu–O2 = 2.2506(9) Å (the largest observed)]. Consequently, the intramolecular copper–copper distance increases to 5.4604(3) Å. The O_{Tf}···O_w (**1**) and Cl···Ow (**4**) hydrogen bonds, very weak C–H···F (**2**), C–H···Cl (**4**) type interactions and π–π stacking (**1**–**5**) contribute to the stabilization of the crystal packing, as analyzed in the Supporting Information (see Figures S2–S6 and Tables S1–S3).

Magnetic Properties and EPR Results

The thermal variation of the magnetic susceptibility per dicopper(II) unit for each compound **1**–**5** is shown in Figures S7–S11. The molar magnetic susceptibility data were corrected for the diamagnetic contribution of the constituent atoms, the temperature independent paramagnetism (TIP) and the sample holder. These magnetic plots are characteristic of antiferromagnetic interactions between two spin doublets, leading to a ground singlet spin state. They were fitted by the Bleaney and Bowers law for a dinuclear copper(II) complex,[44] where the variable parameters are the coupling constant *J* (using the interaction Hamiltonian $\mathbf{H} = -J\,\mathbf{S_1}\cdot\mathbf{S_2}$) and the Landé factor *g*. The least-squares best-fit parameters are listed in Table 1.

Table 1. Best-fit parameters of the thermal variation of the magnetic susceptibility in **1**–**9**.

Compound	J [cm^{-1}]	g	$R \times 10^5$ [a]	Refs.
1	–384	2.17	14	this work
2	–392	2.18	3.1	this work
3	–387	2.19	22	this work
4	–328	2.14	6.3	this work
5	–14.0	2.20	81	this work
6	–386	2.003[b]/2.217[c]	5.4	[42,43]
7	–378	2.00[b]/2.20[c]	6.5	[42]
8	–376	2.01[b]/2.23[c]	7	[42]
9	–385.4	2.216	3.9	[6]

[a] Agreement factor *R* defined as $\Sigma[(\chi_M)_{exp} - (\chi_M)_{calcd}]^2/\Sigma[(\chi_M)_{exp}]^2$. [b] Dinuclear unit. [c] Mononuclear entity.

The X-band EPR spectra of compounds **1**–**5** present broad featureless transitions, centred on *g* values, in line with the susceptibility data (see Table 1). The characteristic weak half-field transition expected for the excited triplet is also observed.

DFT Calculations

DFT calculations were performed using the B3LYP functional (see Computational Details in the Exp. Sect. for further detail). The calculated *J* values are reported in Table 2. They show excellent quantitative agreement with those obtained by the fit of the magnetic data. The calculated magnetic orbitals are shown in Figure 3.[16] The represented orbitals correspond to the empty "magnetic orbitals", because they provide a more accurate description, properly including spin-polarization effects.[45] The analysis of the results and the topology of the bridging ligand clearly indicates that complexes **1**–**4** correspond to the coplanar topology of the $d_{x^2-y^2}$ orbitals in the same plane, with a relatively large overlap, resulting in a strong antiferromagnetic coupling (see calculated magnetic orbitals in Figure 3). This situation is related to the existence of four short Cu–O bridging bond lengths (Table 2). The magnetic orbitals of the two Cu^{II} centres are coplanar (Figure 3). The weaker antiferromagnetic coupling in **4** is due to a relatively large out-of-plane N_2O_2 shift, making the overlap between the two magnetic orbitals less efficient than in **1**–**3**, which have the same topology. Finally, the presence of two long Cu–O bridging bond lengths in complex **5** results in a parallel topology of the two magnetic orbitals.[1] As the overlap between the two magnetic orbitals is much less efficient than in the coplanar topology, there is considerable reduction of the antiferromagnetic interaction (see Table 2).

Table 2. Structural parameters (Cu–O distances and Cu···N_2O_2 plane) of complexes **1**–**5**. Experimental and DFT calculated values of *J*.

Comp.	Cu–O [Å]	Cu···N_2O_2 [Å]	J_{exp} [cm^{-1}]	J_{DFT} [cm^{-1}]
1	1.966, 1.970	0.061	–384	–356
2	1.965, 1965	0.079	–392	–393
3	1.982, 1.981 1.978, 1.972	0.166, 0.177	–387	–384
4	1.988, 1.997	0.410	–328	–296
5	1.966, 2.251	–	–14	–19

We comment below on three points: (i) the large antiferromagnetic singlet–triplet gap |*J*| observed in compounds **1**–**3**, $J \approx (-388 \pm 4)$ cm^{-1}, within experimental uncertainty; (ii) the tuning of the |*J*| value by the chloride ion in **4** to –328 cm^{-1}; and (iii) the important decrease of |*J*| in **5** to –14.0 cm^{-1}, caused by the coordination of the nitrite to the copper(II) ion. The spectacular change of the magnetic exchange coupling between compounds **4** and **5** is illustrated in Figure 2.

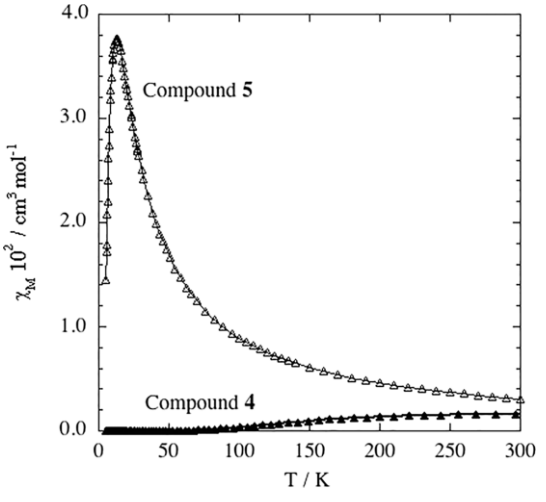

Figure 2. Comparison of the thermal variation of the molar magnetic susceptibility for **4** (full triangles) and **5** (empty triangles). The corresponding curves for **1**–**3** are running below the one of compound **4**; they are not drawn for the sake of clarity (see Figures S7–S9).

(i) We observed in **1**–**3** and in the dinuclear entities **6**–**8** with bpy as the terminal ligand, an antiferromagnetic coupling $J \approx (-388 \pm 4)$ cm^{-1} as large as the one already observed for the dicopper(II) unit $[(tmen)(H_2O)Cu(C_2O_4)Cu(H_2O)(tmen)]^{2+}$[5,6] in **9**, where the bidentate diamine tmen is the end-cap ligand. The geometry of the $N_2Cu(C_2O4)CuN_2$ framework is practically the same in **1**–**3**, **6**–**8** and in **9**. Therefore, we can conclude that the

© 2018 Wiley-VCH Verlag GmbH & Co. KGaA, Weinheim

nature of the diamine terminal ligand has a negligible influence on the value of $|J|$. The interpretation of the coupling (Scheme 2) can be fully extended to the present case. The structural analysis pointed out the presence of different weak intermolecular interactions. The (high temperature) magnetism of **1**–**3**, **6**–**8** and **9** is dominated by the intramolecular magnetic coupling ($|J|$ value). The weak intermolecular interactions play no significant role in the magnetic properties, since at low temperature, the dinuclear complex is a singlet.

The experimental J values and the DFT calculated magnetic orbitals (**1–3** in Figure 3) demonstrate that the axial ligands have a negligible influence on the exchange coupling and that there is no significant mixing of the d_{z^2} orbital in the ground state.

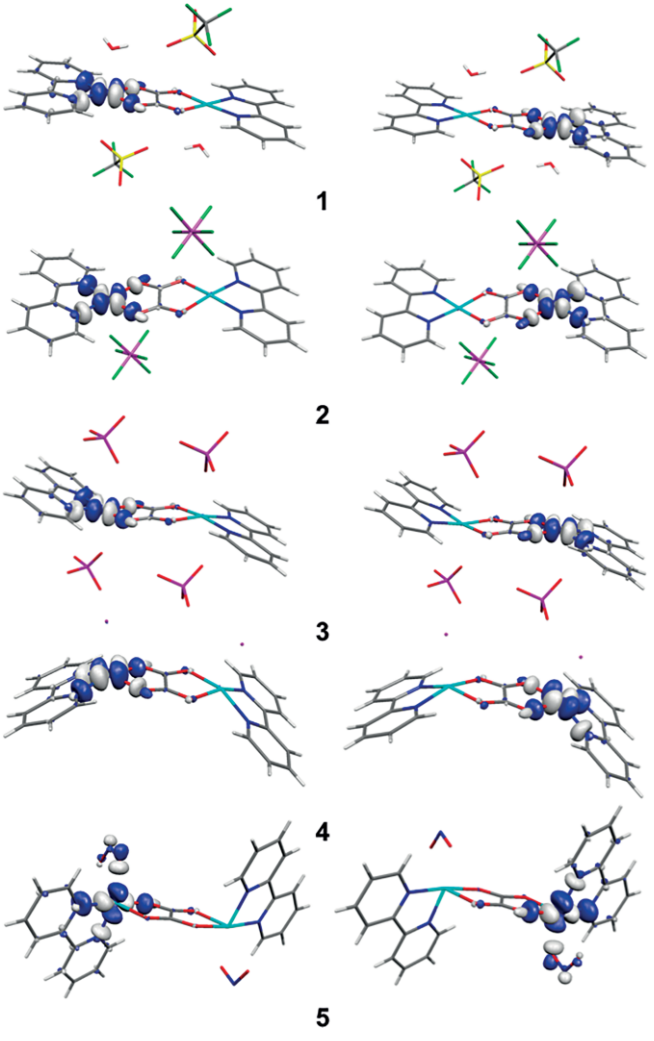

Figure 3. Representation of the magnetic $d_{x^2-y^2}$ orbitals in **1**–**4** and the $d_{z^2-x^2}$ ones in **5** using those bearing the unpaired electrons of the broken-symmetry solutions at a threshold of 0.05 e/Å^3 (see text). The positive lobes are blue, the negative ones are grey. The *x*,*y*,*z* axes are defined in Scheme 1.

(ii) Instead, the decrease of the coupling in **4** is significant, $\Delta|J| \approx -50$ cm^{-1} in **4** compared with **1**–**3** and **9**. This is due to the larger distortion of the bridge in **4**, since DFT calculations show no d_{z^2} orbital admixture in the ground state (**4** in Figure 3). It can be recalled here that Haÿ et al., in a fundamental pioneering work on the mechanism of exchange in dinuclear systems,[38] found a d_{z^2} ground state of the copper(II) ion in the model system $Cl_4Cu(C_2O_4)CuCl_4$ and found a weak d_{z^2}–d_{z^2} interaction and antiferromagnetic coupling. Our previous results[5,11,12,16] and the present work show that this conclusion, obtained with a model geometry, was drawn too quickly.

(iii) The important decrease of the value of $|J|$ in **5** is understood in the frame of the previously described orbital reversal phenomenon, induced by organic ligands.[16–19] Here, it is due to the nitrite anion, which enters the first coordination sphere of the copper(II) ion in a chelating manner, with one short [Cu1–O3 = 2.005 Å] and one long [Cu1–O4 = 2.540 Å] copper–oxygen distance. The CuO_2N_2 basal plane (Cu1O1O3N1N2), defined by the nearest neighbours of the copper centre, becomes almost perpendicular to the oxalate plane [82.01(4)°, Table S3]. The $d_{x^2-y^2}$ magnetic orbital in **1**–**3** switches to $d_{z^2-x^2}$ in **5** (**5** in Figure 3). As already found in ref.[5,6], the oxalate–oxygen O2 in the apical position of the copper(II) ion, presents a Cu1–O2 distance of 2.251 Å, which is longer than the other one (Cu1–O3). There is, therefore, a small admixing of the d_{y^2} magnetic orbital and a small spin density on this O2 oxygen atom. The O2O1 overlap within the two opposite carboxylate bridges becomes weak. The small admixture of the d_{y^2} orbital accounts for the nonzero overlap of the magnetic orbitals. The value of J remains weakly negative, without reaching a positive value, as in the amazing Oshio's ferromagnetic μ-oxalatocopper(II) chain.[40]

Conclusion

We have presented the structure, the magnetic properties and DFT calculations of five dinuclear μ-oxalato dicopper(II) systems. Our data: (i) confirm the peculiar ability of the oxalato bridge to transmit a large antiferromagnetic interaction between two copper(II) ions located at more than 5.1 Å from each other, with a value of J close to –400 cm^{-1} when the two magnetic orbitals overlap strongly through the bridge; (ii) illustrate the significant effect of the counterions on the magnetic properties when they are entering the coordination sphere of the copper(II), with the J values changing from large (–388 cm^{-1}) to weak (–14 cm^{-1}); (iii) reveal good agreement between the experimental and DFT-calculated J values; and (iv) deliver a take-home message for synthetic chemists building sophisticated molecular or supramolecular assemblies: the counterions are not subsidiary components in the synthesis, and they can play a crucial role in both the final structures and the physical properties.

Experimental Section

Materials: Copper(II) salts as triflate, perchlorate hexahydrate, sulfate pentahydrate, chloride dihydrate, 2,2′-bipyridine, oxalic acid dihydrate, lithium(I) hydroxide, barium(II) nitrite and ammonium hexafluorophosphate were purchased from commercial sources and were used as received. The compound $[Cu(bpy)(C_2O_4)]\cdot 2H_2O$ was prepared as described previously.[46a] Copper(II) hexafluorophosphate was generated in solution by using a Lewatit S100 cation-exchange resin as follows: an aqueous solution of copper(II) sulfate pentahydrate (0.4 M) was passed through the column containing the cationic exchange resin in order to replace the protons by cop-

© 2018 Wiley-VCH Verlag GmbH & Co. KGaA, Weinheim

per(II) ions; when the pH of the effluent was the same as that of the initial copper(II) solution, the column was thoroughly washed until no sulfate was detected in the waste. Then, a concentrated aqueous solution (20 mL) of NH_4PF_6 (4 mmol) was allowed to drip slowly into the column and water (50 mL) was used to elute the hexafluorophosphate solution. The eluate (70 mL) containing the copper(II) hexafluorophosphate (4 mmol) was collected to be used in the preparation of **2** (see below). The elemental analyses (C, H, N, Cl, F, P) were performed by the Microanalytical Service of the CNRS (France). A value of 1:1 was determined for the Cu/S (**1**), Cu/P (**2**) and Cu/Cl (**3** and **4**) molar ratios through electron-probe X-ray microanalysis with a Philips XL-30 scanning electron microscope (SEM) from the Central Service for Support to Experimental Research (SCIE) of the Universitat de València.

Safety Note: *The perchlorate salts of complexes with organic ligands are potentially explosive. We worked on the mmol scale and any heating was avoided. Efforts to replace the perchlorate anions by other non-coordinating friendly anions such as triflate are recommended.*

Synthesis of the Complexes

$[Cu_2(bpy)_2(H_2O)_2(C_2O_4)](CF_3SO_3)_2$ (1): Stoichiometric amounts of copper(II) triflate (1 mmol) and bpy (1 mmol) were mixed and dissolved in warm water (75 mL). An aqueous solution containing lithium(I) oxalate (0.5 mmol, 25 mL), generated by mixing LiOH (1 mmol) with oxalic acid (0.5 mmol), was added dropwise under continuous stirring. The resulting sky-blue solution was filtered to remove any small solid particles and it was allowed to evaporate in a fume hood at room temperature. X-ray diffraction quality turquoise-blue needles were grown in a couple of weeks. They were collected by filtration, washed with small amounts of cold water and dried on filter paper. The yield (after collecting the different crops) is practically quantitative. $C_{24}H_{20}Cu_2F_6N_4O_{12}S_2$ (**1**, 861.64): calcd. C 33.46, H 2.31, Cu 14.75, F 13.23, N 6.50; found C 33.25, H 2.24, Cu 14.63, F 13.11, N 6.44.

$[Cu_2(bpy)_2(C_2O_4)](PF_6)_2$ (2): Solid 2,2′-bipyridine (1 mmol) was added to an aqueous solution (120 mL) of copper(II) hexafluorophosphate (1 mmol) under gentle warming and continuous stirring. The addition of lithium(I) oxalate (0.5 mmol, 25 mL) caused an enhancement of the previous sky-blue colour and the resulting solution was allowed to concentrate at room temperature. Deep-blue prisms of **2**, which were suitable for X-ray diffraction were grown within a week, the overall yield being practically quantitative. $C_{22}H_{16}Cu_2F_{12}N_4O_4P_2$ (**2**, 817.41): calcd. C 32.33, H 1.96, Cu 15.55, F 27.90, N 6.85, P 7.58; found C 32.15, H 1.89, Cu 15.10, F 27.75, N 6.76, P 7.47.

$[Cu_2(bpy)_2(C_2O_4)](ClO_4)_2$ (3): The synthesis of **3** followed that of **2**, but used copper(II) perchorate hexahydrate instead of copper(II) hexafluorophosphate and a final volume of 250 mL per 1 mmol of copper(II). X-ray diffraction quality sky-blue prisms of **3** were grown from the blue solution on standing at room temperature after several days. The yield was practically quantitative. $C_{22}H_{16}Cl_2Cu_2N_4O_{12}$ (**3**, 726.39): calcd. C 36.39, H 2.20, Cl 9.76, Cu 17.50, N 7.71; found C 36.28, H 2.16, Cl 9.65, Cu 17.44, N 7.64.

$[Cu_2(bpy)_2Cl_2(C_2O_4)]\cdot H_2O$ (4): Hot water (100 mL) was added to a mixture of $[Cu(bpy)(C_2O_4)]\cdot 2H_2O$, $CuCl_2\cdot 2H_2O$ and 2,2′-bipyridine in a 1:1:1 molar ratio (0.5 mmol of each one) and the resulting suspension was transformed into a sky-blue clear solution by the addition of an aqueous solution of lithium chloride (3 mmol, 25 mL) under continuous stirring. Crystals for X-ray diffraction crystallographic analysis were grown from this solution, as sky-blue sticks, after standing at room temperature for several days. Yield ca. 90. $C_{22}H_{18}Cl_2Cu_2N_4O_5$ (**4**, 616.41): calcd. C 42.88, H 2.92, Cl 11.51, Cu 20.62, N 9.09; found C 42.72, H 2.84, Cl 11.40, Cu 20.45, N 8.99.

The preparation of compound **4** was reported previously by other authors through the oxidation of DMF solutions of $[Cu(bpy)(TSC)_2]X_n$ {TSC = thiosemicarbazide and X = Cl^- (n = 2), $[CuCl_4]^{2-}$ (n = 1)} with hydrogen peroxide, the thiosemicarbazide ligand being rapidly oxidized to oxalate.[46b]

$[Cu_2(bpy)_2(NO_2)_2(C_2O_4)]$ (5): An aqueous solution of copper(II) nitrite (1 mmol) was generated by a metathesis reaction between copper(II) sulfate pentahydrate and barium(II) nitrite in a 1:1 molar ratio. Solid 2,2′-bipyridine was added to the resulting green solution after the removal of the barium(II) sulfate precipitate. Aqueous lithium(I) oxalate (0.5 mmol, 25 mL) and solid $NaNO_2$ (1 mmol) were poured into the previous solution (total volume 100 mL) under continuous stirring. After filtration, to remove any small solid particles, the resulting bright-green aqueous solution was allowed to concentrate at room temperature. X-ray diffraction quality emerald-green prisms of **5** were grown after some days. The yield was practically quantitative. $C_{22}H_{16}Cu_2N_6O_8$ (**5**, 619.50): calcd. C 42.67, H 2.58, Cu 20.52, N 13.56; found C 42.44, H 2.45, Cu 20.39, N 13.43.

Physical Measurements: Magnetic measurements on polycrystalline samples of **1**–**5** were carried out with Faraday-type (**1–3** and **5**) and Quantum Design SQUID MPMXL-5 SQUID (**4**) magnetometers in the temperature range 70–300 K (**1–3**) and 4.0–300 K (**4–5**) under an applied dc magnetic field of 10 kOe. The magnetic susceptibility data were corrected for the diamagnetic contributions of the constituent atoms estimated from Pascal's constants. Corrections for the temperature-independent paramagnetism [120×10^{-3} cm^3 mol^{-1} per two copper(II) ions] and paramagnetic impurities of the sample holder were also applied. X-band EPR spectra on polycrystalline samples of **1**–**5** were performed with a Bruker ER200 spectrometer equipped with a helium continuous-flow cryostat.

X-ray Diffraction Data Collection and Structure Refinement: A single crystal of each compound was selected, mounted onto a cryoloop and transferred in a cold nitrogen-gas stream. Intensity data were collected with a BRUKER Kappa-APEXII diffractometer with graphite-monochromated Mo-K_α radiation (λ = 0.71073 Å). Data collection was performed with APEX2 suite (Bruker). Unit-cell-parameter refinement, integration and data reduction were carried out with SAINT program.[47] SADABS[48] was used for scaling and multiscan absorption corrections. In the WinGX[49] suite of programs, the structures were solved with SHELXS-2013[50] or Sir92[51] programs and were refined by full-matrix least-squares methods using SHELXL-2013.[50] All non-hydrogen atoms were refined anisotropically. The hydrogen atoms were placed at calculated positions and were refined with a riding model. A model of disorder was introduced for the perchlorate anion in **3**. DIAMOND[52] was used to create graphical illustrations.

A summary of the crystal data and refinement conditions for **1**–**5** is given in Table 3, whereas selected data for weak bonds; mean planes and copper surrounding; bond lengths, bond angles and atom–plane distances for these compounds are synoptically displayed in Tables S1, S2 and S3, respectively.

CCDC 1049849 (for **1**), 1049850 (for **2**), 1049851 (for **3**), 1049852 (for **4**) and 1049853 (for **5**) contain the supplementary crystallographic data for this paper. These data can be obtained free of charge from The Cambridge Crystallographic Data Centre.

Computational Details: Electronic-structure calculations, based on density functional theory, provided a good description of the exchange coupling constants, despite the tiny energy differences involved in such parameters. A detailed description of the theoretical

© 2018 Wiley-VCH Verlag GmbH & Co. KGaA, Weinheim

Table 3. Crystal data and details of structure determination for compounds **1**–**5**.

	1	**2**	**3**	**4**	**5**
Chemical formula	$C_{24}H_{20}Cu_2F_6N\,O_{12}S_2$	$C_{22}H_{16}Cu_2F_{12}\,N_4O_4P_2$	$C_{22}H_{16}Cl_2Cu_2N_4O_{12}$	$C_{22}H_{18}Cl_2Cu_2N_4O_5$	$C_{22}H_{16}Cu_2N_6O_8$
Formula mass [g/mol]	861.64	817.41	726.37	616.38	619.49
Z	2	2	2	4	2
T [K]	220	220	220	220	220
Wavelength [Å]	0.71073	0.71073	0.71073	0.71073	0.71073
Crystal system	monoclinic	monoclinic	triclinic	monoclinic	monoclinic
Space group	$P2_1/c$	$C2/m$	$P(-1)$	$C2/c$	$P2_1/n$
a [Å]	8.7631(3)	14.4603(7)	7.1729(5)	18.8399(6)	8.3813(2)
b [Å]	15.3460(5)	13.9152(6)	9.5918(6)	6.7750(2)	11.8051(3)
c [Å]	12.3751(4)	7.8943(4)	19.7996(10)	18.2475(6)	11.8014(3)
α [°]	90	90	82.234(3)	90	90
β [°]	110.547(2)	121.707(1)	80.165(3)	95.135(2)	100.9480(10)
γ [°]	90	90	72.547(4)	90	90
V [Å^3]	1558.32(9)	1351.39(11)	1275.31(14)	2319.77(13)	1146.40(5)
$D_{calcd.}$ [g cm^{-3}]	1.836	2.009	1.892	1.765	1.795
Absorption coefficient [mm^{-1}]	1.603	1.816	1.952	2.107	1.919
θ range [°]	2.20 to 32.13	2.21 to 31.99	2.23 to 30.18	2.17 to 32.05	2.46 to 32.15
Reflections collected/unique	31929/5463	7733/2410	15122/7470	20941/3996	15203/4023
R(int)	0.0214	0.0123	0.0258	0.0141	0.0142
Parameters/restraints	227/0	111/0	397/0	160/0	172/0
R_1 (all data)/wR_2 (all data)	0.0292/0.0737	0.0250/0.0716	0.0594/0.0962	0.0249/0.0632	0.0241/0.0645
R_1 [$I > 2\sigma(I)$]/wR_2 [$I > 2\sigma(I)$]	0.0263/0.0712	0.0240/0.0706	0.0380/0.0880	0.0230/0.0621	0.0215/0.0630
Goodness-of-fit on F^2	0.962	1.084	1.026	1.073	1.067
$\Delta F_{max}/\Delta F_{min}$ [e Å^{-3}]	0.440/–0.518	0.620/–0.499	0.865/–0.544	0.584/–0.305	0.452/–0.323

[a] $R_1 = \Sigma(|F_o| - |F_c|)/\Sigma|F_o|$. [b] $wR_2 = \{\Sigma[w(F_o^2 - F_c^2)^2]/\Sigma[w(F_o^2)^2]\}^{1/2}$ and $w = 1/[\sigma(F_o^2) + (mP)^2 + nP]$ with $P = (F_o^2 + 2F_c^2)/3$, m = 0.0401 (**1**), 0.0389 (**2**), 0.0446 (**3**), 0.0295 (**4**) and 0.0342 (**5**) and n = 1.0816 (**1**), 1.2630 (**2**), 0.5301 (**3**), 2.6304 (**4**) and 0.3775 (**5**).

approach can be found in the literature.[53–57] In the case of the dinuclear complexes, using the experimental geometries in the calculations, the J value was obtained directly from the energy difference between the high-spin state, a triplet state for dinuclear Cu^{II} complexes and the broken-symmetry solution.[53–57] Previously, we studied the effect of the basis set and the choice of the functional on the accuracy of the determination of the exchange coupling constants.[53–57] The calculations were performed using the hybrid B3LYP functional,[58] together with the basis sets proposed by Schaefer et al. We employed a basis set of triple-ζ quality for all atoms[59] and the Gaussian 09 code.[60]

Acknowledgments

We would like to pay tribute to our former supervisor, the regretted late Olivier Kahn, who, a long time ago, suggested the launch of this series of syntheses to check his Heitler and London exchange models in molecules. Over the years, the work was supported by the French-Spanish Picasso Program of the integrated actions program, by the Centre National de la Recherche Scientifique (CNRS) and by the French and Spanish Ministries of Higher Education and Research and the EEC (PCRD Programs). We acknowledge the help of Prof. F. Lloret in magnetic data handling and Prof. S. Alvarez for helpful discussions. E. R. acknowledges Ministerio de Economía y Competitividad (MEC) for the grant CTQ2015-64579-C3-1-P and the computer resources, technical expertise and assistance provided by the CSUC. E. R gives thanks to Generalitat de Catalunya for an ICREA Academia award. M. V. and M. J. are grateful to the Universities of Valencia and Paris 6, respectively, for invitation grants, which provided them with a unique opportunity to complete this work.

Keywords: Copper · Oxalato · Dinuclear complexes · Magnetic properties · Density functional calculations

[1] D. Gatteschi, O. Kahn, R. D. Willett (Eds.), *Magneto-Structural Correlations in Exchanged Coupled Systems*, Reidel, Dordrecht, **1985**.
[2] O. Kahn, *Molecular Magnetism*, VCH Publishers, New York, **1993**.
[3] J.-P. Launay, M. Verdaguer, *Electrons in Molecules: from Basic Principles to Molecular Electronics*, revised ed., Oxford University Press, Oxford, **2018**.
[4] D. Gatteschi, C. Benelli, *Introduction to Molecular Magnetism: From Transition Metals to Lanthanides*, Wiley-VCH, Weinheim, **2015**.
[5] M. Julve, M. Verdaguer, O. Kahn, A. Gleizes, M. Philoche-Levisalles, *Inorg. Chem.* **1983**, *22*, 368–370.
[6] M. Julve, M. Verdaguer, A. Gleizes, M. Philoche-Levisalles, O. Kahn, *Inorg. Chem.* **1984**, *23*, 3808–3818.
[7] M. Julve, C. Train, M. Verdaguer, *Chem. Rev.*, to be published
[8] M. Verdaguer, O. Kahn, M. Julve, A. Gleizes, *Nouv. J. Chim.* **1985**, *9*, 325–334.
[9] F. Lloret, J. Sletten, R. Ruiz, M. Julve, J. Faus, M. Verdaguer, *Inorg. Chem.* **1992**, *31*, 778–784.
[10] M.-C. Dul, E. Pardo, R. Lescouëzec, Y. Journaux, J. Ferrando-Soria, R. Ruiz-García, J. Cano, M. Julve, F. Lloret, D. Cangussu, C. L. M. Pereira, H. O. Stumpf, J. Pasán, C. Ruiz-Pérez, *Coord. Chem. Rev.* **2010**, *254*, 2281–2296.
[11] R. Veit, J.-J. Girerd, O. Kahn, F. Robert, Y. Jeannin, N. El Murr, *Inorg. Chem.* **1984**, *23*, 4448–4454.
[12] J.-J. Girerd, Y. Jeannin, S. Jeannin, O. Kahn, *Inorg. Chem.* **1978**, *17*, 3034–3040.
[13] C. Chauvel, J.-J. Girerd, Y. Jeannin, S. Jeannin, O. Kahn, *Inorg. Chem.* **1979**, *18*, 3015–3020.
[14] R. Vicente, J. Ribas, S. Alvarez, A. Segui, X. Solans, M. Verdaguer, *Inorg. Chem.* **1987**, *26*, 4004–4009.
[15] S. Alvarez, M. Julve, M. Verdaguer, *Inorg. Chem.* **1990**, *29*, 4500–4507.
[16] J. Cano, P. Alemany, S. Alvarez, M. Verdaguer, E. Ruiz, *Chem. Eur. J.* **1998**, *4*, 476–483.
[17] M.-F. Charlot, M. Verdaguer, Y. Journaux, P. De Loth, J.-P. Daudey, *Inorg. Chem.* **1984**, *23*, 3802–3808.
[18] J. J. Girerd, O. Kahn, M. Verdaguer, *Inorg. Chem.* **1980**, *19*, 274–276.

 © 2018 Wiley-VCH Verlag GmbH & Co. KGaA, Weinheim

[19] M. Verdaguer, A. Michalowicz, J.-J. Girerd, N. A. Alberding, O. Kahn, *Inorg. Chem.* **1980**, *19*, 3271–3279.
[20] P. Román, C. Guzmán-Miralles, A. Luque, J. I. Beitia, J. Cano, F. Lloret, M. Julve, S. Alvarez, *Inorg. Chem.* **1996**, *35*, 3741–3751.
[21] M. Julve, M. Verdaguer, M.-F. Charlot, O. Kahn, R. Claude, *Inorg. Chim. Acta* **1984**, *82*, 5–12.
[22] M. Ohba, H. Tamaki, N. Matsumoto, H. Okawa, *Inorg. Chem.* **1993**, *32*, 5385–5390.
[23] Y. Pei, Y. Journaux, O. Kahn, *Inorg. Chem.* **1989**, *28*, 100–103.
[24] M. Verdaguer, M. Julve, A. Michalowicz, O. Kahn, *Inorg. Chem.* **1983**, *22*, 2624–2629.
[25] Z. J. Zhong, N. Matsumoto, H. Okawa, S. Kida, *Chem. Lett.* **1990**, *19*, 87–90.
[26] M. Ohba, H. Tamaki, N. Matsumoto, H. Okawa, S. Kida, *Chem. Lett.* **1991**, *20*, 1157–1160.
[27] H. Tamaki, Z. J. Zhong, N. Matsumoto, S. Kida, M. Koikawa, N. Achiwa, Y. Hashimoto, H. Okawa, *J. Am. Chem. Soc.* **1992**, *114*, 6974–6979.
[28] H. Tamaki, M. Mitsumi, K. Nakamura, N. Matsumoto, S. Kida, H. Okawa, S. Iijima, *Chem. Lett.* **1992**, *21*, 1975–1978.
[29] L. O. Atovmian, G. V. Shilov, R. N. Lyubovskaya, E. L. Zhilyaeva, N. S. Ovanesyan, S. I. Pirumova, I. Gusakovskaya, Y. G. Morozov, *JETP Lett.* **1993**, *58*, 766–769.
[30] S. Decurtins, H. W. Schmalle, P. Schneuwly, J. Ensling, P. Guetlich, *J. Am. Chem. Soc.* **1994**, *116*, 9521–9528.
[31] S. Decurtins, H. W. Schmalle, P. Schneuwly, H. R. Oswald, *Inorg. Chem.* **1993**, *32*, 1888–1892.
[32] S. Decurtins, H. W. Schmalle, H. R. Oswald, A. Linden, J. Ensling, P. Guetlich, A. Hauser, *Inorg. Chim. Acta* **1994**, *216*, 65–73.
[33] C. Mathonière, S. G. Carling, D. Yusheng, P. Day, *J. Chem. Soc., Chem. Commun.* **1994**, 1551–1552.
[34] R. P. Farrell, T. W. Hambley, P. A. Lay, *Inorg. Chem.* **1995**, *34*, 757–758.
[35] A. P. Ginsberg, *Inorg. Chim. Acta Rev.* **1971**, *5*, 45–68.
[36] O. Kahn, B. Briat, *J. Chem. Soc. Faraday Trans. 2* **1976**, *72*, 268–281.
[37] O. Kahn, B. Briat, *J. Chem. Soc. Faraday Trans. 2* **1976**, *72*, 1441–1446.
[38] P. J. Haÿ, J. C. Thibeault, R. Hoffmann, *J. Am. Chem. Soc.* **1975**, *97*, 4884–4899.
[39] R. Cortés, M. K. Urtiaga, L. Lezama, M. I. Arriortua, T. Rojo, *Inorg. Chem.* **1994**, *33*, 829–832.
[40] H. Oshio, U. Nagashima, *Inorg. Chem.* **1992**, *31*, 3295–3301.
[41] J. Shi, G.-M. Yang, P. Cheng, D.-Z. Liao, Z.-H. Jiang, G.-L. Wang, *Polyhedron* **1996**, *16*, 531–534.
[42] A. Gleizes, M. Julve, M. Verdaguer, J. A. Real, J. Faus, X. Solans, *J. Chem. Soc., Dalton Trans.* **1992**, 3209–3216.
[43] M. Julve, J. Faus, M. Verdaguer, A. Gleizes, *J. Am. Chem. Soc.* **1984**, *106*, 8306–8308.
[44] B. Bleaney, K. D. Bowers, *Proc. R. Soc. London Ser. A* **1952**, *214*, 451–465.
[45] T. Cauchy, E. Ruiz, S. Alvarez, *J. Am. Chem. Soc.* **2006**, *128*, 15722–15727.
[46] a) W. Fitzgerald, J. Foley, D. McSweeney, N. Ray, D. Sheahan, S. Tyagi, B. Hathaway, P. O'Brien, *J. Chem. Soc., Dalton Trans.* **1982**, 1117–1121; b) Y. Chattopadhyay, S. Seth, T. C. W. Mak, *J. Coord. Chem.* **2002**, *55*, 259–270.
[47] *SAINT*, v. 2.03, Bruker Analytical X-ray Systems Inc., Madison, WI, USA, **2003**.
[48] *SADABS*, v. 2.03, Bruker Analytical X-ray Systems Inc., Madison, WI, USA, **2000**.
[49] L. J. Farrugia, *J. Appl. Crystallogr.* **1999**, *32*, 837–838.
[50] G. M. Sheldrick, *Acta Crystallogr., Sect. A: Found. Crystallogr.* **2008**, *64*, 112–122.
[51] A. Altomare, G. Cascarano, C. Giacovazzo, A. Guagliardi, M. C. Burla, G. Polidori, M. Camalli, *J. Appl. Crystallogr.* **1994**, *27*, 435.
[52] K. Brandenburg & H. Putz GbR, *Crystal Impact*, Bonn, Germany, **2005**.
[53] E. Ruiz, S. Alvarez, J. Cano, V. Polo, *J. Chem. Phys.* **2005**, *123*, 164110–7.
[54] E. Ruiz, J. Cano, S. Alvarez, P. Alemany, *J. Comput. Chem.* **1999**, *20*, 1391–10.
[55] E. Ruiz, A. Rodríguez-Fortea, J. Cano, S. Alvarez, P. Alemany, *J. Comput. Chem.* **2003**, *24*, 982–989.
[56] E. Ruiz, S. Alvarez, A. Rodríguez-Fortea, P. Alemany, Y. Pouillon, C. Massobrio, "Electronic Structure and Magnetic Behavior in Polynuclear Transition-Metal Compounds" in *Magnetism: Molecules to Materials*, *Vol. 2* (Eds.: J. S. Miller, M. Drillon), Wiley-VCH, Weinheim, **2001**; p. 227–279.
[57] E. Ruiz, A. Rodríguez-Fortea, J. Tercero, T. Cauchy, C. Massobrio, *J. Chem. Phys.* **2005**, *123*, 074102–10.
[58] A. D. Becke, *J. Chem. Phys.* **1993**, *98*, 5648–5652.
[59] A. Schaefer, C. Huber, R. Ahlrichs, *J. Chem. Phys.* **1994**, *100*, 5829–5835.
[60] M. J. Frisch, G. W. Trucks, H. B. Schlegel, G. E. Scuseria, M. A. Robb, J. R. Cheeseman, G. Scalmani, V. Barone, B. Mennucci, G. A. Petersson, H. Nakatsuji, M. Caricato, X. Li, H. P. Hratchian, A. F. Izmaylov, J. Bloino, G. Zheng, J. L. Sonnenberg, M. Hada, M. Ehara, K. Toyota, R. Fukuda, J. Hasegawa, M. Ishida, T. Nakajima, Y. Honda, O. Kitao, H. Nakai, T. Vreven, J. A. Montgomery Jr., J. E. Peralta, F. Ogliaro, M. Bearpark, J. J. Heyd, E. Brothers, K. N. Kudin, V. N. Staroverov, R. Kobayashi, J. Normand, K. Raghavachari, A. Rendell, J. C. Burant, S. S. Iyengar, J. Tomasi, M. Cossi, N. Rega, J. M. Millam, M. Klene, J. E. Knox, J. B. Cross, V. Bakken, C. Adamo, J. Jaramillo, R. Gomperts, R. E. Stratmann, O. Yazyev, A. J. Austin, R. Cammi, C. Pomelli, J. W. Ochterski, R. L. Martin, K. Morokuma, V. G. Zakrzewski, G. A. Voth, P. Salvador, J. J. Dannenberg, S. Dapprich, A. D. Daniels, Ö. Farkas, J. B. Foresman, J. V. Ortiz, J. Cioslowski, D. J. Fox, *Gaussian 09, Revision A.1*, Gaussian, Inc., Wallingford CT, **2009**.

Received: August 2, 2017

© 2018 Wiley-VCH Verlag GmbH & Co. KGaA, Weinheim